D.K. Smith and R.J. Marks II, "Closed form bandlimited image extrapolation",
Applied Optics, vol. 20, pp.2476-2483 (1981).

Closed form bandlimited image extrapolation

David K. Smith and Robert J. Marks II

Digital implementations of a closed form 2-D bandlimited image extrapolation algorithm are presented for a number of elementary target images. The resulting figures of merit empirically verify the assumption that extrapolation is better near to where the image is known. Results of extrapolating a truncated image perturbed by white Gaussian noise suggest a required SNR of the order of 10^{10}.

I. Introduction

In this paper, we present empirical results of the closed form 2-D extrapolation theory developed in Ref. 1, Eq. (15). The algorithm is based on the 1-D extrapolation scheme proposed by Gerchberg,[2] and the corresponding closed form discrete algorithm developed by Sabri and Steenaart.[3] Stated simply, the extrapolation problem is to determine an image everywhere given information about the image over only a finite area. *A priori* knowledge of the image's bandwidth is also assumed.

A number of bandlimited target images were created, and a square $(N \times N)$, $N = 34$ matrix of sample values $\hat{u}$ was formed. A smaller $(m \times m)$ square matrix $\hat{u}_T$ was then used as the truncated image. The extrapolation matrices were formed by the matrix inversion technique described in Sec. 7 of Ref. 1 except that the Hilbert transform low pass matrix[4] was utilized in place of $D^{-1}\hat{G}_{\Omega_\eta}D$, $\eta = x,y$.

Each target function was chosen to explore a particular aspect of the algorithm performance.

II. Figures of Merit

It is desirable to have a figure of merit to quantify the goodness of the extrapolation results. Let $\hat{u}_E$ denote the extrapolation result. One obvious merit comparison is

$$\phi = \frac{(\hat{u}|\hat{u}_E)}{\|\hat{u}\|\|\hat{u}_E\|}, \tag{1}$$

where for real valued matrices

$$(\hat{u}|\hat{u}_E) \equiv \sum_{i,j=0}^{N} \hat{u}(i,j)\hat{u}_E(i,j), \tag{2}$$

and $\|A\|^2 = (A|A)$. From the Cauchy-Schwartz inequality $|\phi| \leq 1$.

This figure of merit, however, is insensitive to the goodness of the extrapolation near the truncated signal. An obvious alteration is to run the inner product summation from the center of the matrix to a $d \times d$ square, where $d \leq N$. The matrices $\hat{u}$ and $\hat{u}_E$, however, are equivalent to u_T within the $m \times m$ square. We remove this bias and write our final figure of merit as

$$\phi(d) = \frac{(\hat{u}|\hat{u}_E)_{m,d}}{\|\hat{u}\|_{m,d}\,\|\hat{u}_E\|_{m,d}}, \tag{3}$$

where

$$(\hat{u}|\hat{u}_E)_{m,d} = \sum_{(m+1)\times(m+1)\text{square}}^{d\times d\ \text{square}} \hat{u}(i,j)\hat{u}_E(i,j),$$

and each square is centered. A value of $\phi(d)$ near unity then dictates a good result. Under the assumption that the extrapolation is better near where the image is known, $\phi(d)$ should be a monotonically decreasing function of d.

III. Implementations

The example implementations to follow are presented in pseudo 3-D plots. The bottom figure in each case corresponds to the target function. The center plot shows the truncated image, and the top plot is the extrapolation result.

A. Example 1

In Fig. 1, the target function is a 2-D sinc function,

$$g(x,y) = \{\sin[2(0.125)(x-17)]\}\{\text{sinc}[2(0.125)(y-17)]\},$$

where $\text{sinc}x = \sin\pi x/\pi x$. The sinc function was found to produce the most accurate reconstruction of any of the functions tried. In this example, the truncation aperture with width $m = 5$ passes less than half of the main lobe of the target sinc. From this the algorithm was able to recreate the target function with very high

The authors are with University of Washington, Department of Electrical Engineering, Seattle, Washington 98195.

Received 21 December 1980
0003-6935/81/142476-08$00.50/0.

accuracy over the entire 34 × 34 region. The figure of merit in Fig. 2 is monotonically decreasing with a minimum value of 0.975.

B. Example 2

This group of figures depicts the extrapolation results for five sequentially shifted off-axis sinc functions. It was desired to see how the extrapolations would vary when different amounts of the signal energy are within the input.

Figure 3 shows the extrapolation result when the center of the target sinc function was located at point (2,32) in the x,y plane. The input is extremely low in energy. The extrapolated output is predictably poor.

In Fig. 1, the target function has been moved closer to the center of the matrix along the diagonal. For this shift and all subsequent ones, the target function was moved three units in the positive x direction and three units in the negative y direction.

Figure 5 shows the result of extrapolating the target sinc which has been moved yet closer to the center along the diagonal. There is still little energy available as input. A pronounced peak is forming toward the northwest corner.

In Fig. 6, the target function has been shifted again. The extrapolated signal is beginning to look very much like the target function. The remarkable thing about this particular extrapolation is its accuracy in view of the small amount of energy that was passed as input. This aspect of extrapolation quality is not reflected in the figures of merit. The final extrapolation in this group is depicted in Fig. 7.

Figure 8 is the figure of merit graph for the five preceding cases. The lines corresponding to Figs. 3 and 4 show better extrapolation close to the truncation aperture than do those corresponding to Figs. 5 and 6. Thus, even though a low percentage of the target function was available, extrapolation near to the truncation is still good. Note that in each case $\phi(d)$ roughly decreases monotonically.

C. Example 3

Recall that the extrapolation process entails an extrapolation along one axis followed by an extrapolation along the other axis. If the input aperture is an $m \times m$ square, for example, the first extrapolation would result in a horizontal or vertical strip of m extrapolated functions centered within the large matrix. The ensuring extrapolation would use those extrapolated values as input. The net result is that the centered vertical strip of width m and the centered horizontal strip of width m in the output matrix are direct extrapolations of the function within the input aperture, while the corners of the output matrix are extrapolations of the first extrapolation.[1] The centered sinc function is a nice signal to extrapolate because most of its structure lies along centered horizontal and vertical bands. The sinc function does not give a good indication of the performance of the algorithm within the corner regions of the matrix, however. Therefore a rotated sinc was used as an input to study the extrapolation in these regions. The rotated sinc has most of its structure within the corner regions and is given by

$$g(x,y) = [\text{sinc2}(0.125)(x - y)][\text{sinc2}(0.125)(x + y - 34)].$$

In Fig. 9, the truncation aperture was a 5 × 5 square which allowed most of the main lobe of the target function through. The area surrounding the main lobe has been reconstructed fairly well, but the corners have been extrapolated poorly. Figure 10 shows the figure of merit calculations for this example. The extrapolation is good over a 12 × 12 square, at which point the quality of the result decays monotonically. As expected, the results are not as good as for the unrotated sinc.

D. Example 4

A target function was created which consisted of a sum of four sinc functions arranged to look like a stylized face. Two sinc functions with equal widths in the x and y dimensions were positioned as eyes, a sinc function elongated in the y direction was centered and represents the nose, and a sinc function broad in the x direction was positioned below center for the mouth. Figure 11 shows the result of this attempt. The input aperture was a 7 × 9 rectangle which passed the nose and part of the mouth. The mouth extrapolated quite nicely. One eye is visible in the extrapolation and, although reproduced in the correct position, it has only about half the amplitude of the target eye.

E. Example 5

Every target function dealt with so far (except the rotated sinc) has been separable in x and y. Thus,

$$\begin{aligned} g(x,y) = {} & [\text{sinc}0.25(x - 17)][\text{sinc}0.25(y - 17)] \\ & + [\text{sinc}0.16(x - y - 4)][\text{sinc } 0.16(x + y - 38)] \\ & + 0.2 \cos[2\pi(x - y)0.06] \end{aligned}$$

was used as a target function. This function consists of a 2-D centered sinc added to a 2-D off-centered rotated sinc and a consinusoid along the diagonal. The spectrum consists of a rect function due to the sinc, an inscribed rotated rect due to the rotated sinc, and two delta functions due to the cosine term. The projection of the spectrum onto the (f_x,f_y) plane is a square. The truncation aperture is a 7 × 7 square.

The resulting extrapolation is shown in Fig. 12. The result is typical in that the area close to the aperture is reproduced well, while the area farther out is not. It appears, however, that the cosine part of the target function has not been reproduced well. The figure of merit for this function is displayed in Fig. 13. It shows that the extrapolation is good over the 16 × 16 square area and then drops off monotonically.

F. Example 6

The low frequency consinusoid part of the target function in the previous example was not reproduced well in the extrapolation. It was decided to test specifically the algorithm performance for low frequency signals by attempting to extrapolate a sinc function on a dc or zero frequency term. A consistent value of −0.6 was added to each sampled value of the sinc function

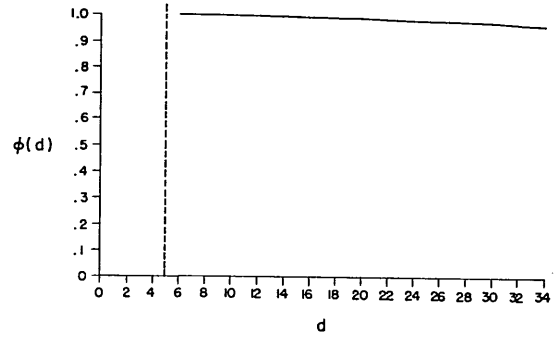

Fig. 2. Figure of merit for the sinc extrapolation in Fig. 1.

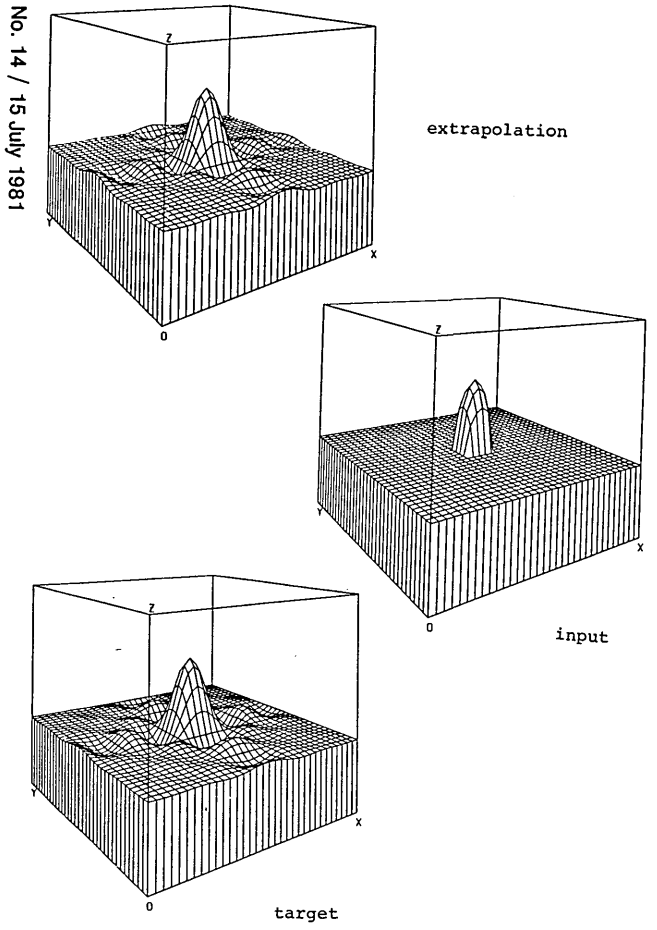

Fig. 1. Extrapolation of a sinc$x$ sinc$y$ function.

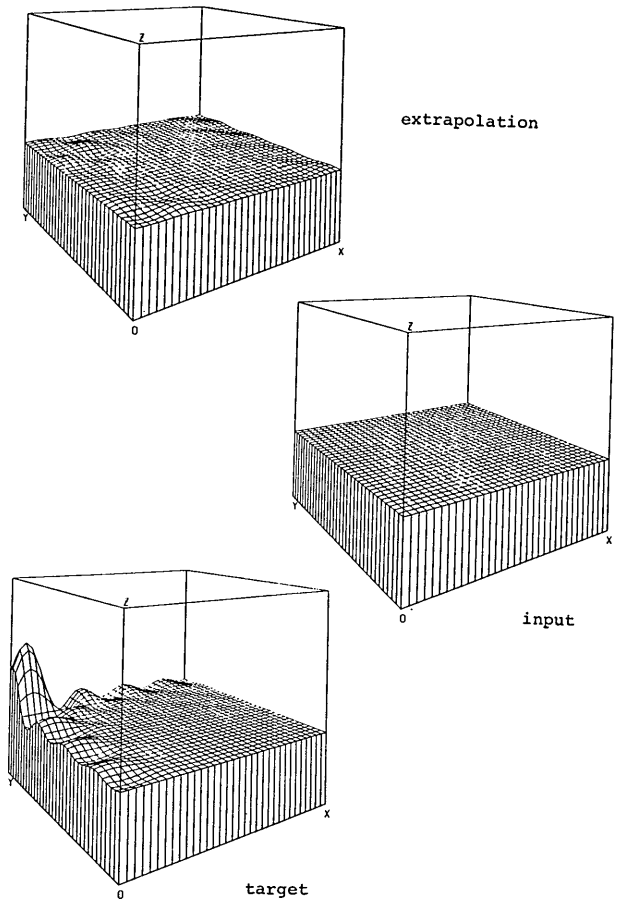

Fig. 3. Extrapolation of a shifted sinc centered at (2,32).

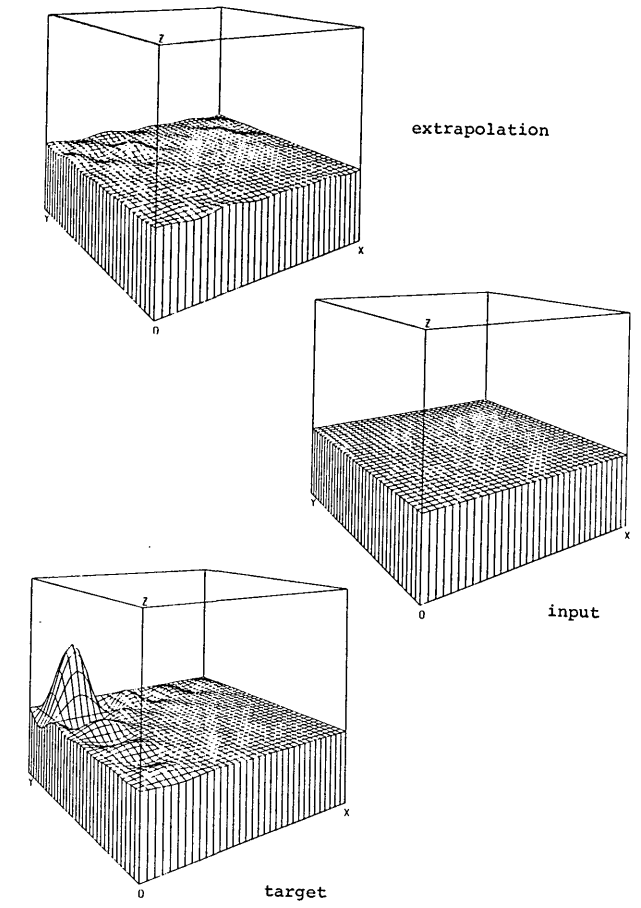

Fig. 4. Extrapolation of a shifted sinc centered at (5,29).

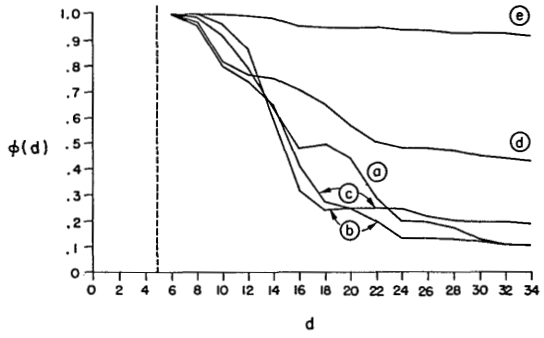

Fig. 8. Figures of merit for the shifted sinc extrapolations in Figs. 3–7.

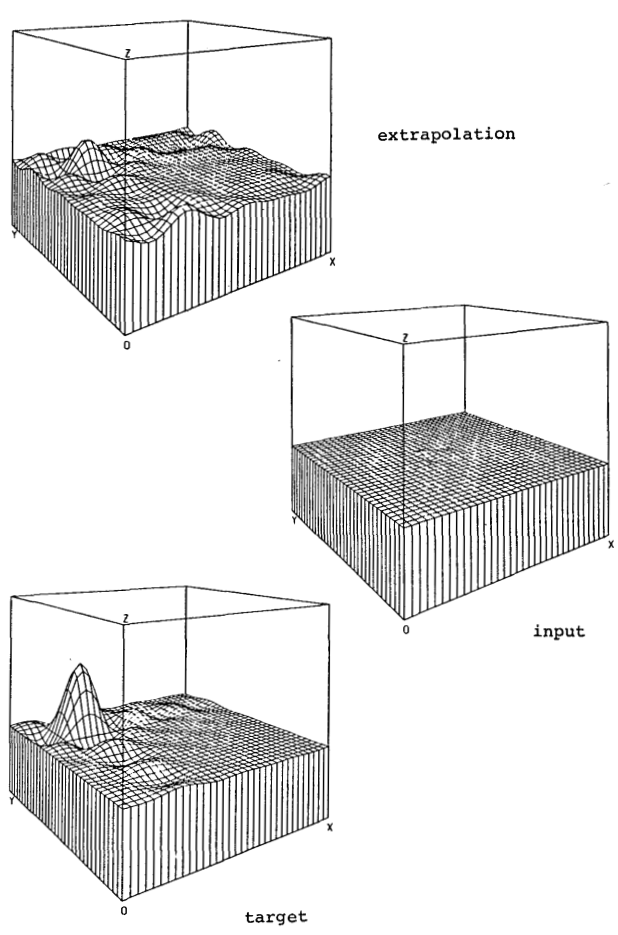

Fig. 5. Extrapolation of a shifted sinc centered at (8,26).

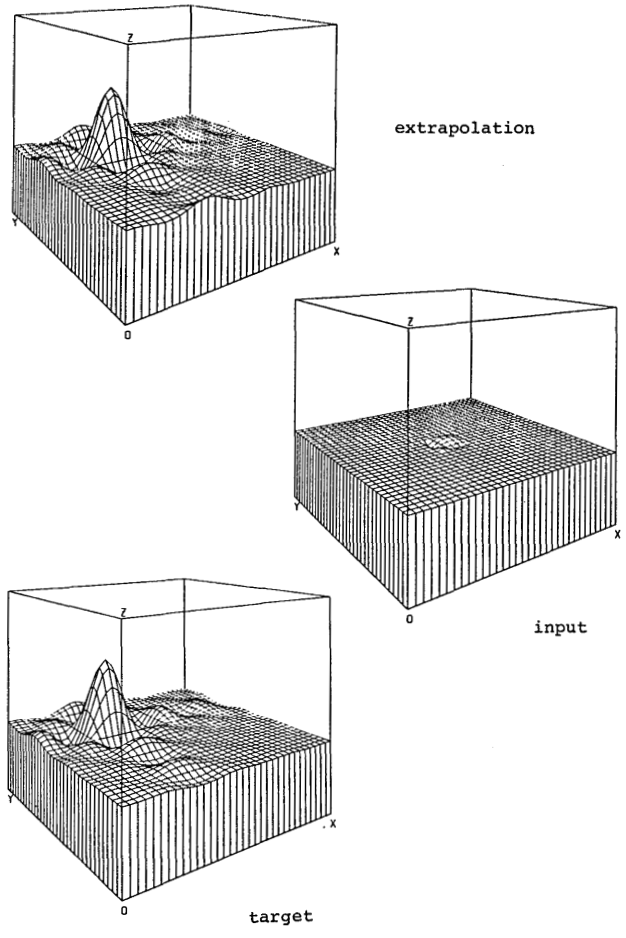

Fig. 6. Extrapolation of a shifted sinc centered at (11,23).

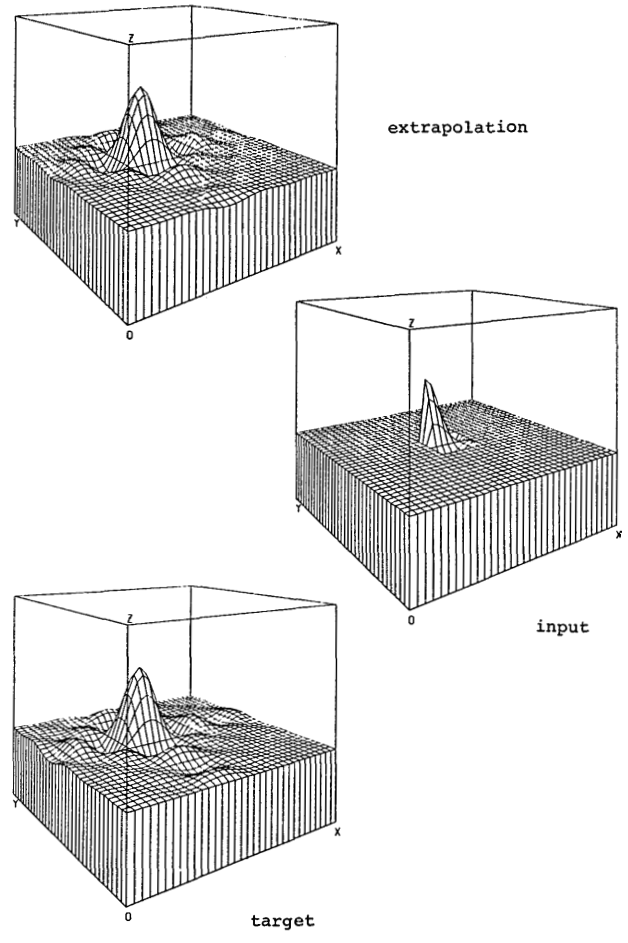

Fig. 7. Extrapolation of a shifted sinc centered at (14,20).

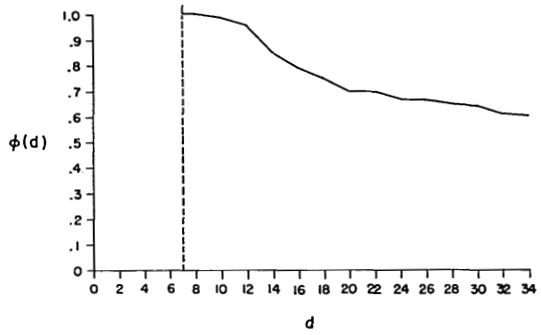

Fig. 10. Figure of merit of the rotated sinc.

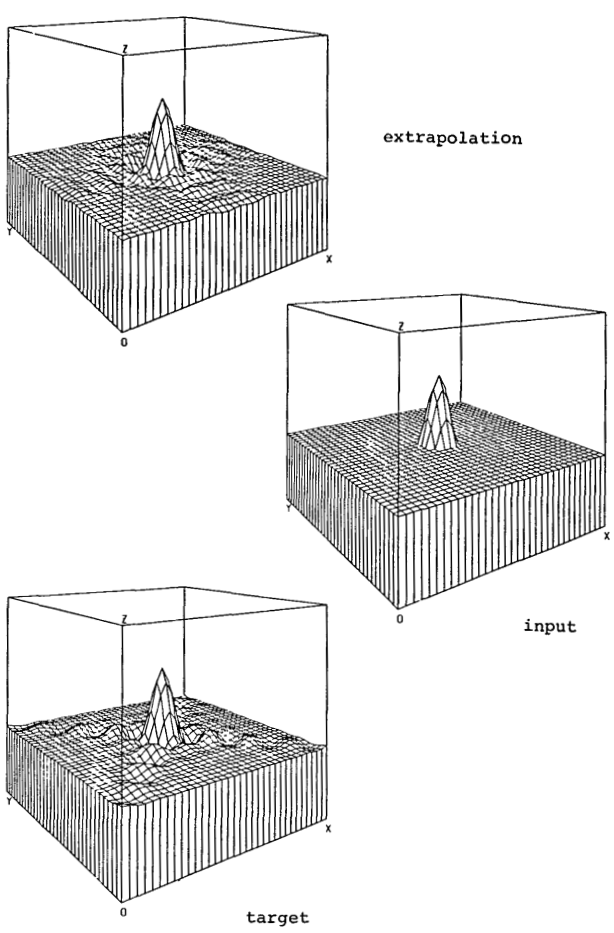

Fig. 9. Extrapolation of a rotated sinc.

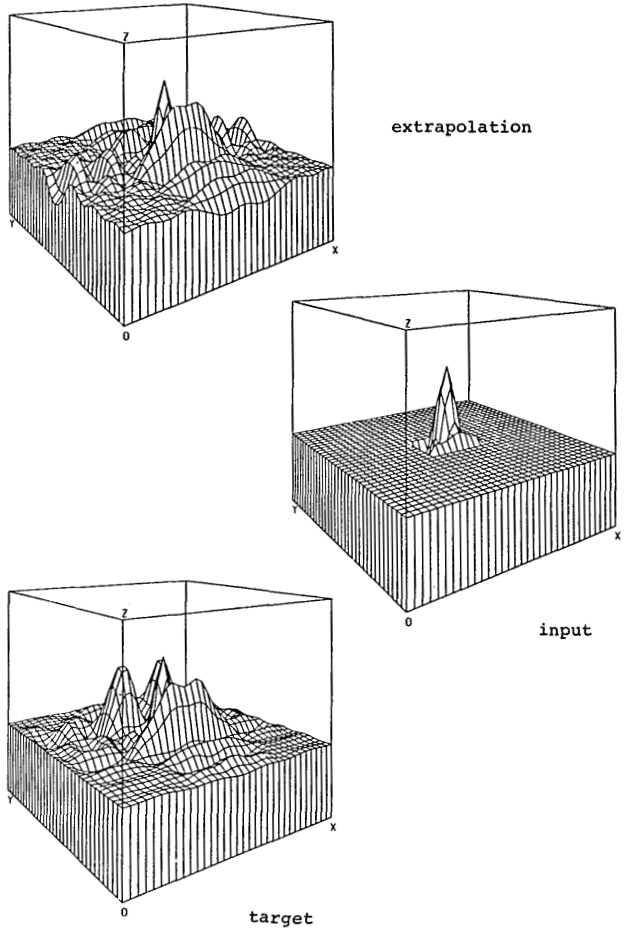

Fig. 11. Extrapolation of a face.

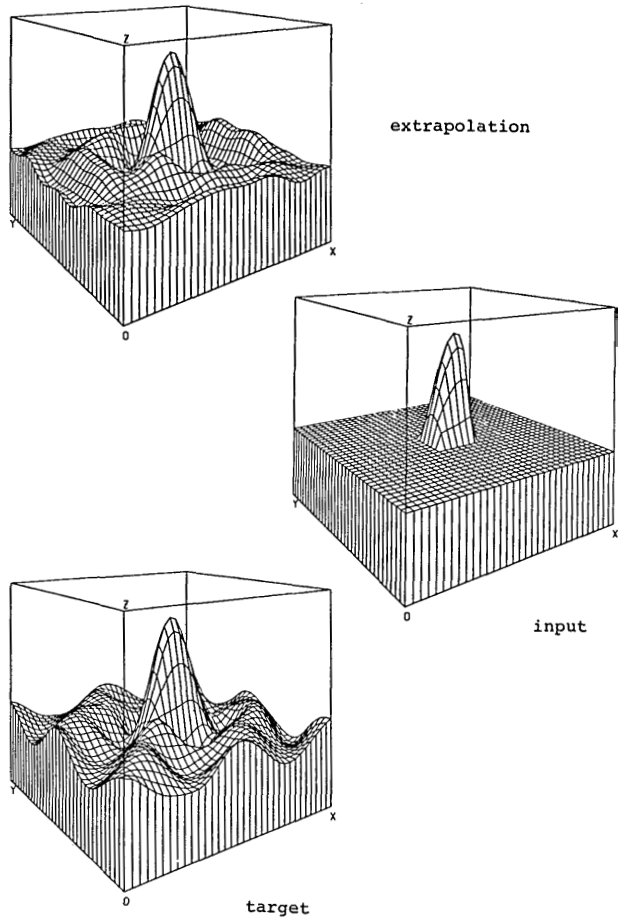

Fig. 12. Extrapolation of a nonseparable image.

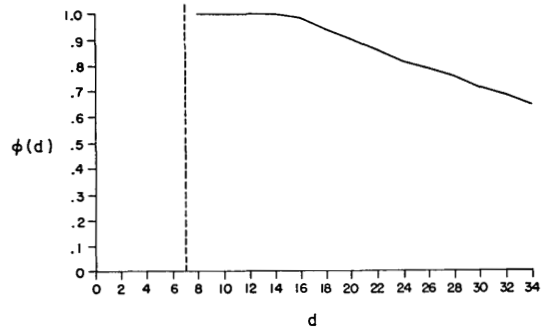

Fig. 13. Figure of merit for the nonseparable image.

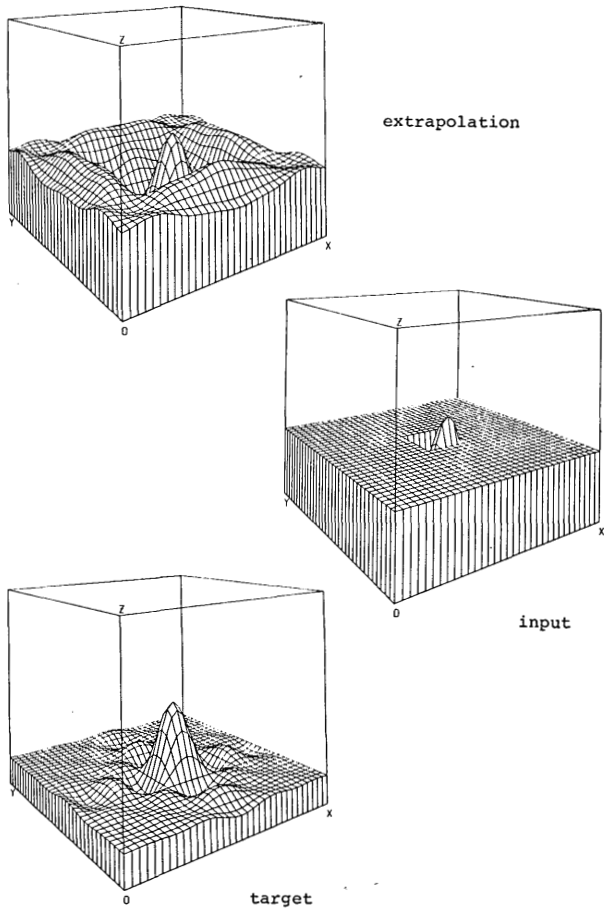

Fig. 14. Extrapolation of a sinc on a DC bias.

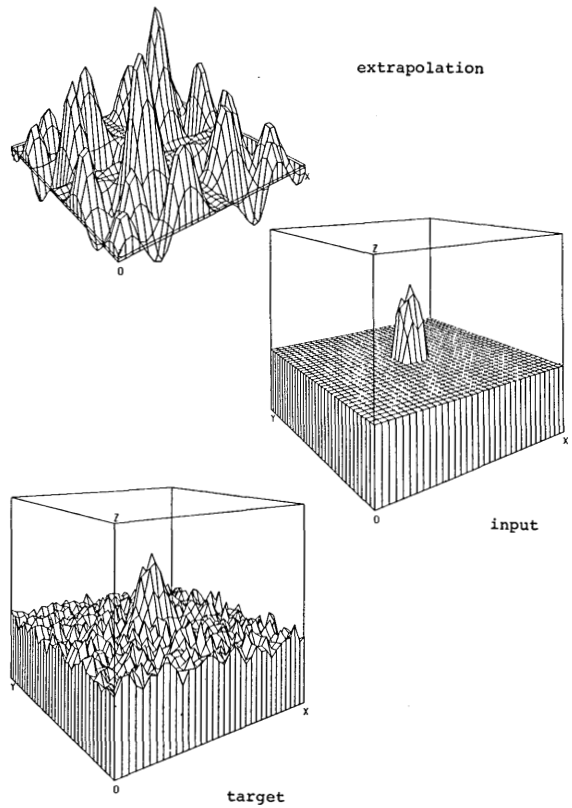

Fig. 15. Extrapolation of a noisy sinc: SNR = 10^2. Note scale change on top figure.

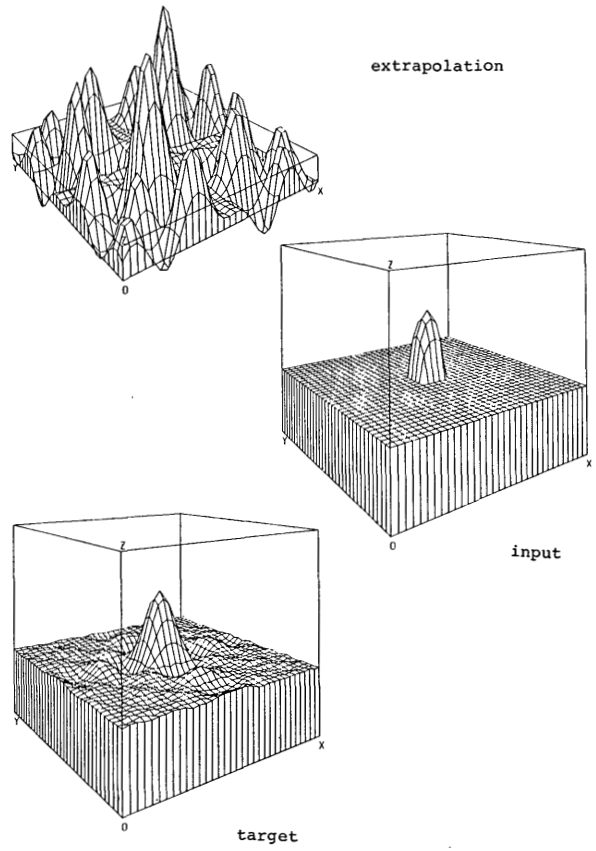

Fig. 16. Extrapolation of a noisy sinc: SNR = 10^4. Note smaller scale change.

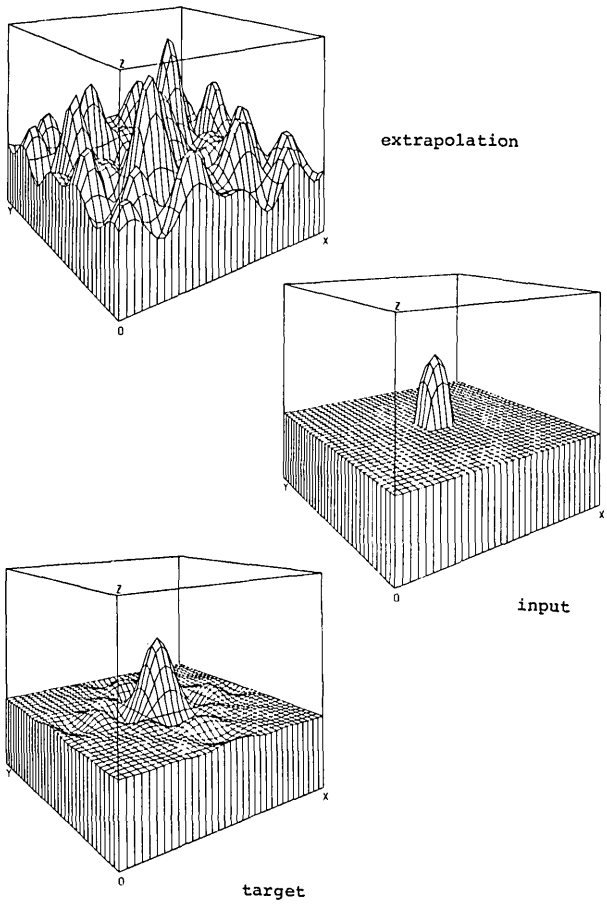

Fig. 17. Extrapolation of a noisy sinc: SNR = 10^6. Equivalent scales.

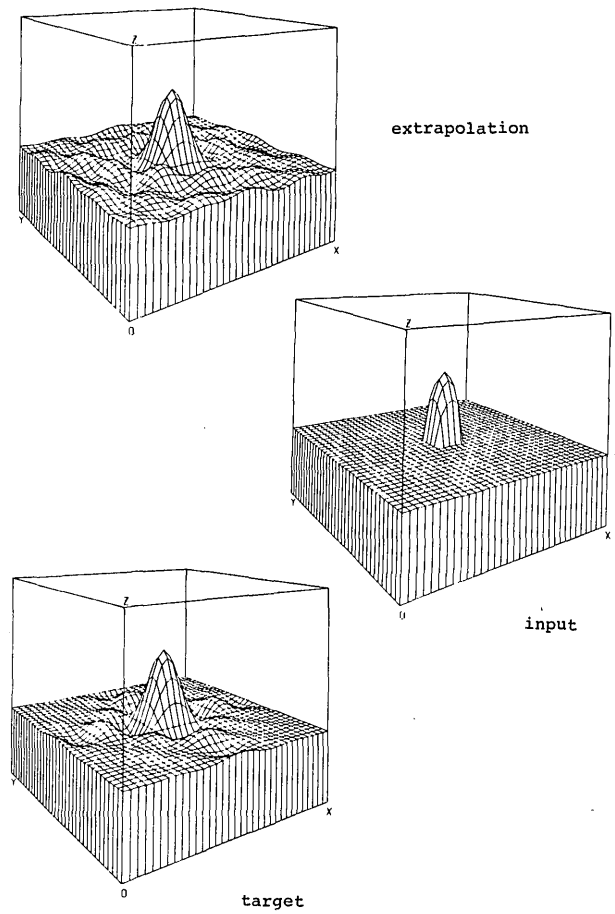

Fig. 18. Extrapolation of a noisy sinc: SNR = 10^8.

and the resulting extrapolation is pictured in Fig. 14. It appears that the algorithm was unable to predict the presence of the bias term. The finite (x,y) aperture does not convey low frequency information well since only a fraction of the periods of these terms can be generated.

G. Example 7

The final set of figures illustrates the performance of the extrapolation algorithm when the input is perturbed by zero mean additive white Gaussian noise. The SNR was changed by specifying different variances for the Gaussian distribution.

In Fig. 15, the output for a sinc perturbed by Gaussian noise is illustrated. The density function of this noise is given by

$$P(\alpha) = \frac{1}{\sqrt{2\pi}\sigma} \exp(-\alpha^2/2\sigma^2),$$

where σ^2 is the variance. The signal to noise power ratio is 100(SNR = $1/\sigma^2$). The input is obviously very distorted, with only the main lobe of the sinc being even partially recognizable. The extrapolated output is extremely poor. Note the scale change caused by the high amplitude peaks in the corners of the output matrix. The horizontal and vertical strips corresponding to the first-order (direct) extrapolation have relatively low amplitude and could possibly be accurate, but the corners corresponding to the second order (indirect) extrapolations are wildly varying. This phenomenon was also found to be characteristic of extrapolations in which the bandwidth had been specified incorrectly. In either case, the noise, which ideally has components at all frequencies, generates an aliasing error.

In Fig. 16, we have the results for a σ of 0.01 and a signal to noise power ratio of 10,000. The input is distorted but substantially less so than in the previous case. The output exhibits the same characteristics as the preceding output, but it could be noted that the scale is different.

Figure 17 shows the result for a standard deviation of 0.001 and a signal to noise power ratio of 10^6. Visibly the input distortion is now undetectable. The output, however, still shows the same distortion as in the first two cases. Again, the amplitude of the output oscillations has decreased.

In Fig. 18, σ is 0.0001, and the signal to noise power ratio has been increased by a factor of 100 to 10^8. The output now is finally starting to look like a sinc.

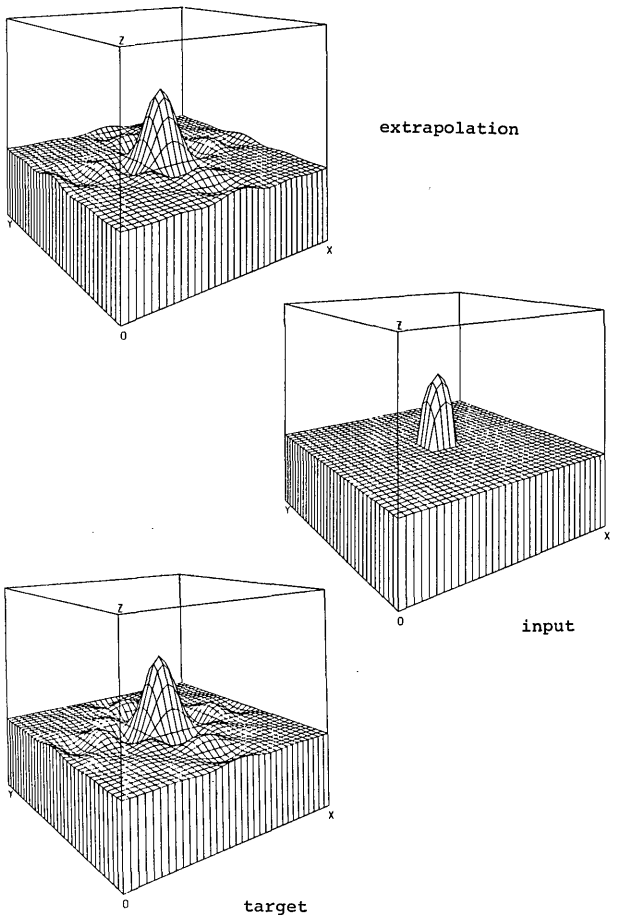

Fig. 19. Extrapolation of a noisy sinc: SNR = 10^{10}.

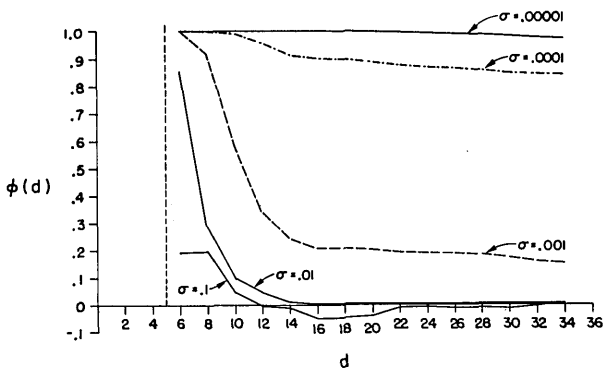

Fig. 20. Figures of merit for the noisy sinc extrapolations in Figs. 15–19.

With a signal to noise power ratio of 10^{10}, the extrapolated output becomes as accurate as that for the unperturbed input in Fig. 1. Figure 19 illustrates this extrapolation.

The figures of merit for the five extrapolations are graphed in Fig. 20. As expected, the more noise the worse the extrapolation.

IV. Conclusions

We have presented a number of implementations of a closed form extrapolation algorithm presented in Ref. 1. The results are supportive of the proposition that extrapolation is better near to where the image is known. The well-established sensitivity of extrapolation algorithms to input noise[5,6] was clearly demonstrated.

This work was generously supported by the National Science Foundation under grant ENG-79-08009.

References

1. R. J. Marks II, Appl. Opt. **20,** 1815 (1981).
2. R. W. Gerchberg, Opt. Acta **21,** 709 (1974).
3. M. S. Sabri and W. Steenaart, IEE Trans. Circuits Syst. **CAS-25,** 74 (1978).
4. M. S. Sabri and W. Steenaart, IEEE Trans. Acoust. Speech Signal Process. **ASSP-25,** 452 (1977).
5. D. C. Youla, IEEE Trans. Circuits Syst. **CAS-25,** 74 (1978).
6. A. Papoulis, IEEE Trans. Circuits Syst. **CAS-22,** 735 (1975).